ELSEVIER

1 March 1999

Physics Letters A 252 (1999) 213-221

PHYSICS LETTERS A

Vlasov-Maxwell description of electron-ion two-stream instability in high-intensity linacs and storage rings

Ronald C. Davidson [a], Hong Qin [a], Tai-Sen F. Wang [b]

[a] *Plasma Physics Laboratory, Princeton University, Princeton, NJ 08543, USA*
[b] *Los Alamos National Laboratory, Los Alamos, NM 87545, USA*

Received 7 October 1998; accepted for publication 22 December 1998
Communicated by M. Porkolab

Abstract

The Vlasov-Maxwell equations are used to investigate properties of the electron-ion two-stream instability for a continuous, high-intensity ion beam propagating in the z-direction with directed axial velocity $V_b = \beta_b c$ through a background population of (stationary) electrons. The analysis is carried out for arbitrary beam intensity, consistent with transverse confinement of the beam particles, and arbitrary fractional charge neutralization by the background electrons. Detailed stability properties are calculated over a wide range of system parameters for dipole perturbations with azimuthal mode number $\ell = 1$. The instability growth rate $\mathrm{Im}\,\omega$ is found to increase with increasing normalized beam intensity $(\hat{\omega}_{pb}^2/\omega_{\beta b}^{0 2})$, increasing fractional charge neutralization $(f = \hat{n}_e/Z_b\hat{n}_b)$, and decreasing proximity of the conducting wall (r_b/r_w). © 1999 Elsevier Science B.V.

PACS: 29.27.Bd; 41.75.-i; 41.85.-p

Periodic focusing accelerators and transport systems [1-3] have a wide range of applications ranging from basic scientific research, to applications such as tritium production, spallation neutron sources, and heavy ion fusion [4,5]. At the high beam currents and charge densities of practical interest, it is increasingly important to develop an improved theoretical understanding of the influence of the intense self-fields produced by the beam space charge and current on detailed equilibrium, stability and transport properties. For a *one-component* high-intensity beam, considerable progress has been made in describing the self-consistent evolution of the beam distribution function $f_b(\boldsymbol{x},\boldsymbol{p},t)$ and the self-generated electric and magnetic fields $\boldsymbol{E}^s(\boldsymbol{x},t)$ and $\boldsymbol{B}^s(\boldsymbol{x},t)$ in kinetic analyses [1,6-10] based on the Vlasov-Maxwell equations. In many practical accelerator applications, however, an (unwanted) second charge component is present. For example, a background population of electrons can result locally when an H^- beam is injected through a stripper foil into a proton storage ring, or when energetic ions strike the chamber wall. When a second charge component is present, it has been recognized for many years, both in theoretical studies and in experimental observations [11-21], that the relative streaming motion of the high-intensity beam particles through the background charge species provides the free energy to drive the classical *two-stream* instability [22,23], appropriately modified to include the effects of dc space charge, relativistic kinematics, presence of a conducting wall, etc. For electrons interacting with a proton beam, as in the Proton Stor-

0375-9601/99/$ - see front matter
PII S0375-9601(99)00002-X

age Ring, the Accelerator for Production of Tritium (APT), or the Spallation Neutron Source (SNS), this instability is usually referred to as the electron–proton (e–p) instability [15–17], although a similar instability also exists for other ion species, including (for example) electron–ion interactions in electron storage rings [18–21], or in high-intensity ion beams for heavy ion fusion [5].

Theoretical treatments of the electron–ion two-stream instability are traditionally based on models (see, for example, Refs. [11–13,15–17]) that analyze the center-of-mass motion of the ion and electron charge components. Such models, while treating accurately several bulk features of the instability, are limited in scope and difficult to generalize to include the dependence of stability behavior on the detailed phase-space properties of the distribution functions. Therefore, in the present analysis, we develop and apply a theoretical formalism based on the Vlasov–Maxwell equations [1,24] that describe the self-consistent interaction of the ion and electron distribution functions with the applied field and the self-generated electric and magnetic fields. Furthermore, in integrating the linearized Vlasov–Maxwell equations, we make use of the method of characteristics [23,24] to integrate along the particle trajectories in the equilibrium field configuration. Finally, apart from requiring transverse confinement of the beam particles by the focusing field, no a priori restriction is made on ion beam intensity. The analysis can be applied to ion beams ranging from the emittance-dominated, moderate-intensity proton beams in present and next-generation proton linacs and storage rings, to the low-emittance, space-charge-dominated ion beams in heavy ion fusion.

The present analysis considers a high-intensity ion beam with distribution function $f_b(\boldsymbol{x},\boldsymbol{p},t)$, and characteristic radius r_b and axial momentum $\gamma_b m_b \beta_b c$ propagating in the z-direction through a background population of electrons with distribution function $f_e(\boldsymbol{x},\boldsymbol{p},t)$. The ions have high directed axial velocity $V_b = \beta_b c$ in the z-direction, and the background electrons are assumed to be nonrelativistic and stationary with $\int d^3p\, p_z f_e \simeq 0$ in the laboratory frame. In the smooth-beam approximation, the ion beam is assumed to be continuous in the z-direction, and the *applied* transverse focusing force on a beam ion is modeled by

$$\boldsymbol{F}^{b}_{foc} = -\gamma_b m_b \omega^{0^2}_{\beta b} \boldsymbol{x}_\perp, \tag{1}$$

where $\boldsymbol{x}_\perp = x\hat{\boldsymbol{e}}_x + y\hat{\boldsymbol{e}}_y$ is the transverse displacement, $(\gamma_b - 1)m_b c^2$ is the characteristic ion kinetic energy, m_b is the ion rest mass, c is the speed of light in vacuo, and $\omega^0_{\beta b}$ = const is the effective betatron frequency for transverse ion motion in the applied focusing field. For the background electrons, assuming that the ion density exceeds the background electron density, the space-charge force on an electron, $\boldsymbol{F}^s_e = e\nabla\phi$, provides transverse confinement of the background electrons by the electrostatic potential $\phi(\boldsymbol{x},t)$. It is further assumed that the ion motion in the beam frame is nonrelativistic, and that the transverse momentum components of the beam ions and the characteristic spread in axial momentum are small compared with the directed axial momentum, i.e., $|p_x|, |p_y|, |\delta p_z| \ll \gamma_b m_b \beta_b c$. The space-charge intensity in the present analysis is allowed to be arbitrarily large, subject only to transverse confinement of the beam ions by the focusing force in Eq. (1).

In addition, the present analysis is carried out in the electrostatic approximation, where the self-generated electric field produced by space-charge effects is $\boldsymbol{E}^s(\boldsymbol{x},t) = -\nabla\phi(\boldsymbol{x},t)$, and the electrostatic potential $\phi(\boldsymbol{x},t)$ is determined self-consistently from Poisson's equation

$$\nabla^2\phi = -4\pi e(Z_b n_b - n_e). \tag{2}$$

Here, $n_b(\boldsymbol{x},t) = \int d^3p\, f_b(\boldsymbol{x},\boldsymbol{p},t)$ and $n_e(\boldsymbol{x},t) = \int d^3p\, f_e(\boldsymbol{x},\boldsymbol{p},t)$ are the ion and electron number densities, respectively. To determine the self-generated magnetic field $\boldsymbol{B}^s(\boldsymbol{x},t) = \nabla A_z(\boldsymbol{x},t) \times \hat{\boldsymbol{e}}_z$ produced by the axial ion current, it is assumed that the axial velocity profile $V_{zb}(\boldsymbol{x},t) \simeq \beta_b c$ is approximately *uniform* over the beam cross section. In this case, in the magnetostatic approximation, the z-component of vector potential $A_z(\boldsymbol{x},t)$ is determined self-consistently from

$$\nabla^2 A_z = -4\pi Z_b e \beta_b n_b, \tag{3}$$

where use is made of the assumption that the electrons carry zero axial current in the laboratory frame.

Finally, under *equilibrium* conditions ($\partial/\partial t = 0$), the present analysis assumes that ion and electron properties are spatially uniform in the z-direction with $\partial/\partial z = 0$. However, the *stability* analysis assumes small-amplitude perturbations with z- and t-variations proportional to $\exp(ik_z z - i\omega t)$, where $k_z = 2\pi n/L$ is the axial wavenumber, and ω is the (complex) oscillation frequency, with $\mathrm{Im}\,\omega > 0$ corresponding to instability. Here, n is an integer, L is the fundamental axial periodicity length of perturbed quantities in straight (e.g., linac) geometry, and $L = 2\pi R$ for the case of a storage ring with (large) radius $R \gg r_b$. For present purposes, the stability analysis assumes perturbations with sufficiently long axial wavelength and high frequency that $k_z^2 r_b^2 \ll 1$, $|\omega/k_z - \beta_b c| \gg v_{Tbz}$, and $|\omega/k_z| \gg v_{Tez}$. Here, $v_{Tbz} = (2T_{bz}/\gamma_b m_b)^{1/2}$ and $v_{Tez} = (2T_{ez}/m_e)^{1/2}$ are the characteristic axial thermal speeds of the beam ions and the background electrons, respectively. These inequalities lead to several simplifications. For example, because $k_z^2 r_b^2 \ll 1$, the three-dimensional Laplacian ∇^2 occurring in Eqs. (2) and (3) can be approximated by $\nabla_\perp^2 = \partial^2/\partial x^2 + \partial^2/\partial y^2$. Furthermore, the perturbed axial forces, e.g., $\delta \boldsymbol{F}_e = e(\partial/\partial z)\delta\phi\hat{\boldsymbol{e}}_z$ and $\delta \boldsymbol{F}_b = -Z_b e(\partial/\partial z)\delta\phi\hat{\boldsymbol{e}}_z$, are treated as negligibly small. The subsequent analysis therefore neglects the effects of Landau damping (by resonant particles) due to the axial momentum spread [23].

We make use of the assumptions summarized above to simplify the theoretical model based on the Vlasov–Maxwell equations [25]. First, we introduce the reduced distribution functions defined by $F_b(\boldsymbol{x}, \boldsymbol{p}_\perp, t) = \int dp_z\, f_b(\boldsymbol{x}, \boldsymbol{p}, t)$, and $F_e(\boldsymbol{x}, \boldsymbol{p}_\perp, t) = \int dp_z\, f_e(\boldsymbol{x}, \boldsymbol{p}, t)$. Because $\int dp_z\, p_z f_e \simeq 0$ for the electrons, and axial forces are treated as negligibly small, the nonlinear Vlasov equation for $F_e(\boldsymbol{x}, \boldsymbol{p}_\perp, t)$ is given (nonrelativistically) by

$$\left\{\frac{\partial}{\partial t} + \frac{\boldsymbol{p}_\perp}{m_e}\cdot\frac{\partial}{\partial \boldsymbol{x}_\perp} + (e\nabla_\perp\phi)\cdot\frac{\partial}{\partial \boldsymbol{p}_\perp}\right\}F_e(\boldsymbol{x}, \boldsymbol{p}_\perp, t) = 0, \tag{4}$$

where $-e$ is the electron charge, and $\nabla_\perp \equiv \hat{\boldsymbol{e}}_x\partial/\partial x + \hat{\boldsymbol{e}}_y\partial/\partial y$ is the perpendicular gradient. The ions, however, have large directed axial velocity $V_b \simeq \beta_b c$. Therefore, we approximate $\boldsymbol{v}\cdot\partial/\partial\boldsymbol{x} \simeq (\boldsymbol{p}_\perp/\gamma_b m_b)\cdot\partial/\partial\boldsymbol{x}_\perp + V_b\partial/\partial z$, and the perpendicular self-field force on an ion is approximated by $\boldsymbol{F}_{b\perp} \simeq Z_b e[-\nabla_\perp\phi + \beta_b\hat{\boldsymbol{e}}_z \times (\nabla_\perp A_z \times \hat{\boldsymbol{e}}_z)]$, where ϕ and A_z are determined self-consistently from Eqs. (2) and (3). The Vlasov equation for $F_b(\boldsymbol{x}, \boldsymbol{p}_\perp, t)$ then becomes

$$\left\{\frac{\partial}{\partial t} + V_b\frac{\partial}{\partial z} + \frac{\boldsymbol{p}_\perp}{\gamma_b m_b}\cdot\frac{\partial}{\partial \boldsymbol{x}_\perp} - (\gamma_b m_b \omega_{\beta b}^{0\,2}\boldsymbol{x}_\perp + Z_b e\nabla_\perp\psi)\cdot\frac{\partial}{\partial \boldsymbol{p}_\perp}\right\}F_b(\boldsymbol{x}, \boldsymbol{p}_\perp, t) = 0. \tag{5}$$

Here, $+Z_b e$ is the ion charge, and $\psi(\boldsymbol{x}, t)$ is the combined potential defined by $\psi(\boldsymbol{x}, t) \equiv \phi(\boldsymbol{x}, t) - \beta_b A_z(\boldsymbol{x}, t)$. The self-field potentials $\phi(\boldsymbol{x}, t)$, and $\psi(\boldsymbol{x}, t)$ solve

$$\left(\frac{\partial^2}{\partial x^2} + \frac{\partial^2}{\partial y^2}\right)\phi = -4\pi e\left(Z_b\int d^2p\, F_b - \int d^2p\, F_e\right), \tag{6}$$

$$\left(\frac{\partial^2}{\partial x^2} + \frac{\partial^2}{\partial y^2}\right)\psi = -4\pi e\left(\frac{Z_b}{\gamma_b^2}\int d^2p\, F_b - \int d^2p\, F_e\right), \tag{7}$$

where we have approximated $\nabla^2 \simeq \nabla_\perp^2 = \partial^2/\partial x^2 + \partial^2/\partial y^2$.

Eqs. (4)–(7) constitute a complete description of the collective interaction of the beam ions with the background electrons based on the Vlasov–Maxwell equations. In the subsequent analysis, we further assume that the beam propagates axially through a perfectly conducting cylindrical pipe with radius $r = r_w$. Enforcing $[E_\theta^s]_{r=r_w} = [E_z^s]_{r=r_w} = [B_r^s]_{r=r_w} = 0$ readily gives $\phi(r = r_w, \theta, z, t) = 0$, and $\psi(r = r_w, \theta, z, t) = 0$. Here, the constant values of the potentials at $r = r_w$ have been taken equal to zero.

Under quasisteady equilibrium conditions with $\partial/\partial t = 0$, we assume axisymmetric beam propagation ($\partial/\partial\theta = 0$) and negligible variation with axial coordinate ($\partial/\partial z = 0$). It is readily shown from Eqs. (4)–(7) that the equilibrium distribution functions ($\partial/\partial t = 0$) for the beam ions and background electrons are of the general form $F_b^0 = F_b^0(H_{\perp b})$ and $F_e^0 = F_e^0(H_{\perp e})$, where $H_{\perp b}$ and $H_{\perp e}$ are the single-particle Hamiltonians defined by

$$H_{\perp b} = \frac{1}{2\gamma_b m_b}p_\perp^2 + \tfrac{1}{2}\gamma_b m_b \omega_{\beta b}^{0\,2} r^2 + Z_b e[\psi^0(r) - \hat{\psi}^0],$$
$$H_{\perp e} = \frac{1}{2m_e}p_\perp^2 - e[\phi^0(r) - \hat{\phi}^0]. \tag{8}$$

Here, for $\partial/\partial\theta = 0 = \partial/\partial z$, $H_{\perp b}$ and $H_{\perp e}$ are exact single-particle constants of the motion, and the constants $\hat{\psi}^0 \equiv \psi^0(r = 0)$ and $\hat{\phi}^0 \equiv \phi^0(r = 0)$ are the on-axis ($r = 0$) values of $\psi^0(r)$ and $\phi^0(r)$.

There is wide latitude in specifying the functional forms of the equilibrium distribution functions [10]. Once $F_b^0(H_{\perp b})$ and $F_e^0(H_{\perp e})$ are specified, however, the equilibrium self-field potentials and density profiles can be calculated self-consistently from Eqs. (6) and (7) with $\partial/\partial\theta = 0 = \partial/\partial z$. For example, for the thermal equilibrium distributions $F_j^0(H_{\perp j}) = \beta_j \exp(-H_{\perp j}/T_{\perp j})$, where $j = \mathrm{b,e}$, and β_j and $T_{\perp j}$ are positive constants, it can be shown that the density profiles, $n_j^0(r) = \int d^2p\, F_j^0(H_{\perp j})$, for the ions and electrons are bell-shaped and vary continuously with radial coordinate r [25]. On the other hand, for monoenergetic ions and electrons, with distribution functions [24-26]

$$F_b^0(H_{\perp b}) = \frac{\hat{n}_b}{2\pi\gamma_b m_b}\delta(H_{\perp b} - \hat{T}_{\perp b}),$$
$$F_e^0(H_{\perp e}) = \frac{\hat{n}_e}{2\pi m_e}\delta(H_{\perp e} - \hat{T}_{\perp e}), \tag{9}$$

it is found that the density profiles $n_j^0(r)$, $j = \mathrm{b,e}$, correspond to overlapping step-function profiles. Here, $\hat{n}_b$ and $\hat{n}_e \equiv fZ_b\hat{n}_b$ are positive constants corresponding to the ion and electron densities, $f = \mathrm{const}$ is the fractional charge neutralization, and $\hat{T}_{\perp b}$ and $\hat{T}_{\perp e}$ are constants corresponding to the on-axis ($r = 0$) values of the transverse ion and electron temperatures, respectively. Without presenting details [25], some algebraic manipulation of Eqs. (6)-(9) gives the step-function density profiles $n_j^0(r) = \hat{n}_j = \mathrm{const}$, for $0 \leqslant r < r_b$, and $n_j^0(r) = 0$ for $r_b < r \leqslant r_w$, and $j = \mathrm{b,e}$. Here, the beam radius r_b is related to other equilibrium parameters by $\hat{\nu}_b^2 r_b^2 = 2\hat{T}_{\perp b}/\gamma_b m_b$ and $\hat{\nu}_e^2 r_b^2 = 2\hat{T}_{\perp e}/m_e$, where for monoenergetic ions and electrons, the (depressed) betatron frequencies $\hat{\nu}_b$ and $\hat{\nu}_e$ are defined by

$$\hat{\nu}_b^2 = \omega_{\beta b}^{0^2} - \tfrac{1}{2}\left(\frac{1}{\gamma_b^2} - f\right)\hat{\omega}_{pb}^2 = \mathrm{const},$$
$$\hat{\nu}_e^2 = \tfrac{1}{2}\frac{\gamma_b m_b}{Z_b m_e}(1 - f)\hat{\omega}_{pb}^2 = \mathrm{const}, \tag{10}$$

where $\hat{\omega}_{pb}^2 = 4\pi\hat{n}_b Z_b^2 e^2/\gamma_b m_b$ is the ion plasma frequency-squared. The inequalities, $\hat{\nu}_b^2 > 0$ and $\hat{\nu}_e^2 > 0$, are required for existence of the equilibrium. Therefore, we obtain the inequalities $(\hat{\omega}_{pb}^2/\omega_{\beta b}^{0^2})(1 - \gamma_b^2 f) < 2\gamma_b^2$ and $f < 1$, as restrictions on beam intensity and fractional charge neutralization for transverse confinement of the ions and electrons.

For small-amplitude perturbations about general equilibrium distributions, $F_b^0(H_{\perp b})$ and $F_e^0(H_{\perp e})$, and corresponding self-field potentials, $\psi^0(r)$ and $\phi^0(r)$, a stability analysis proceeds by linearizing Eqs. (4)-(7). Perturbed quantities are expressed as $\delta\psi(\boldsymbol{x},t) = \delta\hat{\psi}(\boldsymbol{x}_\perp)\exp(ik_z z - i\omega t)$, $\delta F_b(\boldsymbol{x},\boldsymbol{p}_\perp,t) = \delta\hat{F}_b(\boldsymbol{x}_\perp,\boldsymbol{p}_\perp)\exp(ik_z z - i\omega t)$, etc., where $\boldsymbol{x}_\perp = (x,y)$, and $\mathrm{Im}\,\omega > 0$ is assumed, corresponding to instability (temporal growth). The linearized Vlasov equations are formally integrated by using the method of characteristics [24,25] to integrate along the unperturbed trajectories, $\boldsymbol{x}'_\perp(t')$ and $\boldsymbol{p}'_\perp(t')$, in the equilibrium field configuration. Some straightforward algebra that makes use of Eqs. (4)-(7) gives

$$\delta\hat{F}_e(\boldsymbol{x}_\perp,\boldsymbol{p}_\perp) = -e\frac{\partial}{\partial H_{\perp e}}F_e^0(H_{\perp e})\Bigg\{\delta\hat{\phi}(\boldsymbol{x}_\perp) + i\omega\int_{-\infty}^{0} d\tau\,\delta\hat{\phi}(\boldsymbol{x}'_\perp)\exp(-i\omega\tau)\Bigg\}, \tag{11}$$

$$\delta\hat{F}_b(\boldsymbol{x}_\perp,\boldsymbol{p}_\perp) = Z_b e\frac{\partial}{\partial H_{\perp b}}F_b^0(H_{\perp b})\Bigg\{\delta\hat{\psi}(\boldsymbol{x}_\perp) + i(\omega - k_z V_b)\int_{-\infty}^{0} d\tau\,\delta\hat{\psi}(\boldsymbol{x}'_\perp) \times \exp[-i(\omega - k_z V_b)\tau]\Bigg\}, \tag{12}$$

where the potential amplitudes, $\delta\hat{\phi}(\boldsymbol{x}_\perp)$ and $\delta\hat{\psi}(\boldsymbol{x}_\perp)$, are related to $\delta\hat{F}_e(\boldsymbol{x}_\perp,\boldsymbol{p}_\perp)$ and $\delta\hat{F}_b(\boldsymbol{x}_\perp,\boldsymbol{p}_\perp)$ by

$$\left(\frac{\partial^2}{\partial x^2} + \frac{\partial^2}{\partial y^2}\right)\delta\hat{\phi} = -4\pi e\left[Z_b\int d^2p\,\delta\hat{F}_b - \int d^2p\,\delta\hat{F}_e\right], \tag{13}$$

$$\left(\frac{\partial^2}{\partial x^2} + \frac{\partial^2}{\partial y^2}\right)\delta\hat{\psi} = -4\pi e\left[\frac{1}{\gamma_b^2}Z_b\int d^2p\,\delta\hat{F}_b - \int d^2p\,\delta\hat{F}_e\right]. \tag{14}$$

In Eqs. (11) and (12), $\tau = t' - t$ is the displaced time variable, and the 'primed' orbits, $\boldsymbol{x}'_\perp(t')$ and $\boldsymbol{p}'_\perp(t')$, in the equilibrium field configuration are taken to pass through the phase-space point $(\boldsymbol{x}_\perp,\boldsymbol{p}_\perp)$ at time $t' =$

t [24,25]. For example, for the ion orbit $\boldsymbol{x}'_\perp(t')$ occurring in the eigenfunction $\delta\hat{\psi}(\boldsymbol{x}'_\perp)$ in Eq. (12), the transverse displacement $\boldsymbol{x}'_\perp(t')$ solves

$$\frac{\mathrm{d}^2}{\mathrm{d}t'^2}\boldsymbol{x}'_\perp(t') + \left[\omega_{\beta\mathrm{b}}^{0^2} + \frac{Z_\mathrm{b}e}{\gamma_\mathrm{b}m_\mathrm{b}r'}\frac{\partial}{\partial r'}\psi^0(r')\right]\boldsymbol{x}'_\perp(t') = 0, \tag{15}$$

subject to the boundary conditions $\boldsymbol{x}'_\perp(t'=t) = \boldsymbol{x}_\perp$ and $[\mathrm{d}\boldsymbol{x}'_\perp(t')/\mathrm{d}t']_{t'=t} = \boldsymbol{p}_\perp/\gamma_\mathrm{b}m_\mathrm{b}$. Here, $r'(t') = [x'^2(t') + y'^2(t')]^{1/2}$. The electron orbit $\boldsymbol{x}'_\perp(t')$ occurring in the eigenfunction $\delta\hat{\phi}(\boldsymbol{x}'_\perp)$ in Eq. (11), solves an equation identical in form to Eq. (15) provided we make the replacements $Z_\mathrm{b}e \to -e$, $\psi^0(r') \to \phi^0(r')$, $\gamma_\mathrm{b}m_\mathrm{b} \to m_\mathrm{e}$, and $\omega_{\beta\mathrm{b}}^{0^2} \to 0$ in Eq. (15).

The kinetic eigenvalue equations (11)–(14) have a wide range of applicability, and can be used to determine the complex oscillation frequency ω and detailed stability properties for a wide range of system parameters and choices of equilibrium distribution functions $F_\mathrm{b}^0(H_{\perp\mathrm{b}})$ and $F_\mathrm{e}^0(H_{\perp\mathrm{e}})$ [25]. The principal challenge in analyzing Eqs. (11)–(14) is two-fold. First, depending on the equilibrium profiles, the transverse orbits $\boldsymbol{x}'_\perp(t')$ are often difficult to calculate in closed analytical form. Second, once the orbits in the equilibrium fields are determined, the integrations over t' in Eqs. (11) and (12) are challenging because the orbits occur explicitly in the arguments of the (yet unknown) eigenfunction amplitudes $\delta\hat{\phi}(\boldsymbol{x}'_\perp)$ and $\delta\hat{\psi}(\boldsymbol{x}'_\perp)$.

For present purposes, we specialize to the choice of *monoenergetic* ion and electron distributions in Eq. (9), and the corresponding step-function equilibrium density profiles with $n_j^0(r) = \hat{n}_j = \text{const}$, for $0 \leqslant r < r_\mathrm{b}$, and $n_j^0(r) = 0$, for $r_\mathrm{b} < r \leqslant r_\mathrm{w}$. In this case, $\psi^0(r) - \hat{\psi}^0$ and $\phi^0(r) - \hat{\phi}^0$ are proportional to r^2 in the beam interior $(0 \leqslant r < r_\mathrm{b})$, and the ion orbit equation (15) can be integrated exactly to give

$$\boldsymbol{x}'_\perp(t') = \boldsymbol{x}_\perp\cos(\hat{\nu}_\mathrm{b}\tau) + \frac{1}{\gamma_\mathrm{b}m_\mathrm{b}\hat{\nu}_\mathrm{b}}\boldsymbol{p}_\perp\sin(\hat{\nu}_\mathrm{b}\tau) \tag{16}$$

for $0 \leqslant r'(t') < r_\mathrm{b}$. Here, $\tau = t' - t$ and $\hat{\nu}_\mathrm{b}$ is the (depressed) betatron frequency defined in Eq. (10). The electron orbit $\boldsymbol{x}'_\perp(t')$ is identical in form to Eq. (16), provided we make the replacements $\gamma_\mathrm{b}m_\mathrm{b} \to m_\mathrm{e}$ and $\hat{\nu}_\mathrm{b} \to \hat{\nu}_\mathrm{e}$ in Eq. (16). A careful examination of the eigenvalue equations (11)–(14) for the choice of equilibrium distributions in Eq. (9) [25] shows that Eqs. (11)–(14) support a class of *exact* solutions in which the perturbed potentials have the forms $\delta\hat{\psi}(\boldsymbol{x}_\perp) = \delta\hat{\psi}_\ell(r)\exp(\mathrm{i}\ell\theta) = \hat{\psi}_\ell r^\ell\exp(\mathrm{i}\ell\theta)$ and $\delta\hat{\phi}(\boldsymbol{x}_\perp) = \delta\hat{\phi}_\ell(r)\exp(\mathrm{i}\ell\theta) = \hat{\phi}_\ell r^\ell\exp(\mathrm{i}\ell\theta)$ in the beam interior $(0 \leqslant r < r_\mathrm{b})$. Here, $\hat{\psi}_\ell$ and $\hat{\phi}_\ell$ are constant amplitudes, ℓ is the azimuthal mode number, and we have introduced cylindrical polar coordinates (r,θ) defined by $x = r\cos\theta$ and $y = r\sin\theta$. In carrying out the integration over transverse momentum in Eqs. (13) and (14), we express $\int\mathrm{d}p_x\int\mathrm{d}p_y\ldots = \int_0^\infty\mathrm{d}p_\perp p_\perp\int_0^{2\pi}\mathrm{d}\varphi\ldots$, where $p_x = p_\perp\cos\varphi$, $p_y = p_\perp\sin\varphi$, $p_\perp = (p_x^2+p_y^2)^{1/2}$, and φ is the phase of $\boldsymbol{p}_\perp$ in the transverse plane. To evaluate the perturbed ion and electron charge densities on the right-hand side of Eqs. (13) and (14), what is required are the orbit integrals occurring in Eqs. (11) and (12) averaged over the perpendicular momentum phase φ. For example, for perturbations with azimuthal mode number ℓ, we express $\delta\hat{\psi}(\boldsymbol{x}'_\perp) = \delta\hat{\psi}_\ell(r')\exp(\mathrm{i}\ell\theta') = \hat{\psi}_\ell r'^\ell\exp(\mathrm{i}\ell\theta')$ for $0 \leqslant r' < r_\mathrm{b}$ in the ion orbit integral occurring in Eq. (12). Making use of Eq. (16) and $r'^\ell\exp(\mathrm{i}\ell\theta') = [x' + \mathrm{i}y']^\ell$, the required phase-averaged ion orbit integral can be evaluated in closed analytical form to give [14,25]

$$\begin{aligned} I_\mathrm{b}^\ell(\boldsymbol{x}_\perp,p_\perp) &\equiv \mathrm{i}(\omega - k_zV_\mathrm{b})\hat{\psi}_\ell \\ &\times \int_{-\infty}^{0}\mathrm{d}\tau\exp\{-\mathrm{i}(\omega - k_zV_\mathrm{b})\tau\} \\ &\times \int_0^{2\pi}\frac{\mathrm{d}\varphi}{2\pi}[x'(t') + \mathrm{i}y'(t')]^\ell \\ &= -\frac{1}{2^\ell}\sum_{m=0}^{\ell}\frac{\ell!}{m!(\ell-m)!} \\ &\times \frac{\omega - k_zV_\mathrm{b}}{\omega - k_zV_\mathrm{b} - (\ell-2m)\hat{\nu}_\mathrm{b}}\delta\hat{\psi}(\boldsymbol{x}_\perp), \end{aligned} \tag{17}$$

for $0 \leqslant r < r_\mathrm{b}$. From Eqs. (11) and (13), the corresponding electron orbit integral $I_\mathrm{e}^\ell(\boldsymbol{x}_\perp,p_\perp)$ is identical in form to Eq. (17), provided we make the replacements $\omega - k_zV_\mathrm{b} \to \omega$, $\hat{\nu}_\mathrm{b} \to \hat{\nu}_\mathrm{e}$, and $\delta\hat{\psi}(\boldsymbol{x}_\perp) \to \delta\hat{\phi}(\boldsymbol{x}_\perp) = \delta\hat{\phi}_\ell(r)\exp(\mathrm{i}\ell\theta) = \hat{\phi}_\ell r^\ell\exp(\mathrm{i}\ell\theta)$ in Eq. (17). Finally, for the choice of distribution functions in Eq. (9), it can be shown that

$$2\pi\int_0^\infty dp_\perp\, p_\perp \frac{\partial}{\partial H_{\perp b}} F_b^0(H_{\perp b}) = -\frac{\hat{n}_b}{\gamma_b m_b \hat{\nu}_b^2 r_b}\delta(r-r_b), \quad (18)$$

with an analogous expression for the electrons, making the replacements $H_{\perp b} \to H_{\perp e}$, $\hat{n}_b \to \hat{n}_e$, $\gamma_b m_b \to m_e$, and $\hat{\nu}_b^2 \to \hat{\nu}_e^2$.

Making use of Eqs. (17) and (18), and the electron analogues, we evaluate the perturbed ion and electron densities, occurring in the linearized Maxwell equations (13) and (14). For perturbations with azimuthal mode number ℓ, we express $\delta\hat{\psi}(\boldsymbol{x}_\perp) = \delta\hat{\psi}_\ell(r)\exp(i\ell\theta)$ and $\delta\hat{\phi}(\boldsymbol{x}_\perp) = \delta\hat{\phi}_\ell(r)\exp(i\ell\theta)$, and Eqs. (13) and (14) reduce to

$$\left(\frac{1}{r}\frac{\partial}{\partial r}r\frac{\partial}{\partial r} - \frac{\ell^2}{r^2}\right)\delta\hat{\phi}^\ell(r) = \left[\frac{\hat{\omega}_{pb}^2}{\hat{\nu}_b^2}\Gamma_b^\ell(\omega - k_z V_b)\,\delta\hat{\psi}^\ell(r) + \frac{\hat{\omega}_{pe}^2}{\hat{\nu}_e^2}\Gamma_e^\ell(\omega)\,\delta\hat{\phi}^\ell(r)\right]\frac{1}{r_b}\delta(r-r_b), \quad (19)$$

and

$$\left(\frac{1}{r}\frac{\partial}{\partial r}r\frac{\partial}{\partial r} - \frac{\ell^2}{r^2}\right)\delta\hat{\psi}^\ell(r) = \left[\frac{\hat{\omega}_{pb}^2}{\gamma_b^2\hat{\nu}_b^2}\Gamma_b^\ell(\omega - k_z V_b)\,\delta\hat{\psi}^\ell(r) + \frac{\hat{\omega}_{pe}^2}{\hat{\nu}_e^2}\Gamma_e^\ell(\omega)\,\delta\hat{\phi}^\ell(r)\right]\frac{1}{r_b}\delta(r-r_b). \quad (20)$$

Here, $\hat{\omega}_{pe}^2 = 4\pi\hat{n}_e e^2/m_e$, and the ion and electron susceptibilities are defined by

$$\Gamma_b^\ell(\omega - k_z V_b) = -\frac{1}{2^\ell}\sum_{m=0}^{\ell}\frac{\ell!}{m!(\ell-m)!} \times \frac{(\ell-2m)\hat{\nu}_b}{(\omega - k_z V_b) - (\ell-2m)\hat{\nu}_b},$$

$$\Gamma_e^\ell(\omega) = -\frac{1}{2^\ell}\sum_{m=0}^{\ell}\frac{\ell!}{m!(\ell-m)!}\,\frac{(\ell-2m)\hat{\nu}_e}{\omega - (\ell-2m)\hat{\nu}_e}, \quad (21)$$

for general azimuthal harmonic number ℓ. Note that the perturbed charge and current densities on the right-hand sides of Eqs. (19) and (20) correspond to perturbations localized to the beam surface at $r = r_b$. Therefore, the *exact* solutions for $\delta\hat{\psi}_\ell(r)$ and $\delta\hat{\phi}_\ell(r)$ are proportional to r^ℓ for $0 \leqslant r < r_b$, and proportional to r^ℓ and $r^{-\ell}$ for $r_b < r \leqslant r_w$. We enforce continuity of the perturbed potentials at $r = r_b$, and $\delta\hat{\psi}_\ell(r = r_w) = 0 = \delta\hat{\phi}_\ell(r = r_w)$ at the perfectly conducting wall. We further relate the discontinuities in $\partial\delta\phi_\ell/\partial r$ and $\partial\delta\psi_\ell/\partial r$ at $r = r_b$ by integrating Eqs. (19) and (20) across the beam surface at $r = r_b$. Some algebraic manipulation, which is summarized elsewhere [25], gives the kinetic dispersion relation

$$\left[\frac{2}{1-(r_b/r_w)^{2\ell}} + \frac{\hat{\omega}_{pb}^2}{\ell\gamma_b^2\hat{\nu}_b^2}\Gamma_b^\ell(\omega - k_z V_b)\right] \times \left[\frac{2}{1-(r_b/r_w)^{2\ell}} + \frac{\hat{\omega}_{pe}^2}{\ell\hat{\nu}_e^2}\Gamma_e^\ell(\omega)\right] = \frac{\hat{\omega}_{pe}^2}{\ell\hat{\nu}_e^2}\cdot\frac{\hat{\omega}_{pb}^2}{\ell\hat{\nu}_b^2}\Gamma_e^\ell(\omega)\,\Gamma_b^\ell(\omega - k_z V_b). \quad (22)$$

Eq. (22) is the final form of the kinetic dispersion relation, derived from the linearized Vlasov–Maxwell equations for small-amplitude perturbations about the monoenergetic equilibrium distributions in Eq. (9) and the corresponding step-function density profiles. As such, Eq. (22) can be used to determine the complex oscillation frequency ω over a wide range of system parameters, including normalized beam intensity $(\hat{\omega}_{pb}^2/\omega_{\beta b}^{02})$, fractional charge neutralization $(f = \hat{n}_e/Z_b\hat{n}_b)$, azimuthal mode number (ℓ), axial wavenumber (k_z), etc., subject only to the simplifying assumptions summarized earlier in this paper. In the absence of electrons $(\hat{n}_e = 0)$, the dispersion relation (22) supports purely stable $(\mathrm{Im}\,\omega = 0)$ collective oscillations of the ion beam, and reveals a rich harmonic content at frequencies $\omega - k_z V_b = \pm\hat{\nu}_b, \pm 2\hat{\nu}_b, \ldots, \pm\ell\hat{\nu}_b$. When background electrons are present $(\hat{n}_e \neq 0)$, however, Eq. (22) supports unstable solutions $(\mathrm{Im}\,\omega > 0)$ with instability resulting from the axial streaming $(V_b \neq 0)$ of the beam ions through the background electrons.

A careful examination of Eq. (22) for $\hat{n}_e \neq 0$ shows that the strongest instability (largest growth rate) occurs for azimuthal mode number $\ell = 1$, corresponding to a simple (dipole) displacement of the beam ions and the background electrons. For $\ell = 1$, we find $\Gamma_e^1(\omega) = -\hat{\nu}_e^2/[\omega^2 - \hat{\nu}_e^2]$ and $\Gamma_b^1(\omega - k_z V_b) = -\hat{\nu}_b^2/[(\omega - k_z V_b)^2 - \hat{\nu}_b^2]$ from Eq. (21), and introduce the electron and ion collective oscillation frequencies, ω_e and ω_b, defined by

$$\omega_e^2 \equiv \hat{\nu}_e^2 + \tfrac{1}{2}\hat{\omega}_{pe}^2\left(1-\frac{r_b^2}{r_w^2}\right) = \tfrac{1}{2}\frac{\gamma_b m_b}{Z_b m_e}\hat{\omega}_{pb}^2\left(1-f\frac{r_b^2}{r_w^2}\right),$$
$$\omega_b^2 \equiv \hat{\nu}_b^2 + \frac{\hat{\omega}_{pb}^2}{2\gamma_b^2}\left(1-\frac{r_b^2}{r_w^2}\right) = \omega_{\beta b}^{0^2} + \tfrac{1}{2}\hat{\omega}_{pb}^2\left(f-\frac{1}{\gamma_b^2}\frac{r_b^2}{r_w^2}\right), \quad (23)$$

where $\hat{\omega}_{pe}^2$ has been expressed as $\hat{\omega}_{pe}^2 = (\gamma_b m_b/Z_b m_e) f \hat{\omega}_{pb}^2$. Substituting into Eq. (22) and rearranging terms, the $\ell = 1$ dispersion relation can be expressed in the compact form

$$[(\omega - k_z V_b)^2 - \omega_b^2][\omega^2 - \omega_e^2] = \omega_f^4, \quad (24)$$

where ω_f is defined by

$$\omega_f^4 \equiv \tfrac{1}{4} f\left(1-\frac{r_b^2}{r_w^2}\right)^2 \frac{\gamma_b m_b}{Z_b m_e}\hat{\omega}_{pb}^4. \quad (25)$$

In the absence of background electrons ($f = 0$ and $\omega_f = 0$), Eq. (24) gives stable collective oscillations of the ion beam with frequency $\omega - k_z V_b = \pm\omega_b$, where ω_b is defined in Eq. (23). For $f \neq 0$, however, the ion and electron terms on the left-hand side of Eq. (24) are coupled by the ω_f^4 term on the right-hand side, leading to one unstable solution with $\mathrm{Im}\,\omega > 0$ for a certain range of axial wavenumber k_z. The instability is two-stream in nature, and results from the directed ion motion with axial velocity V_b through the (stationary) background electrons. Eq. (24) is a fourth-order algebraic equation for the complex oscillation frequency ω. Some straightforward analysis shows that there are two stable solutions to Eq. (24) with purely real ω, and two complex solutions for a certain range of k_z that are complex conjugates (one is growing with $\mathrm{Im}\,\omega > 0$, and the other is damped with $\mathrm{Im}\,\omega < 0$). Eq. (24) can of course be solved numerically for ω over a wide range of system parameters. In this regard, it is important to recognize that the dispersion relation (24) is applicable over a wide range of normalized beam intensity $(\hat{\omega}_{pb}^2/\omega_{\beta b}^{0^2})$ and fractional charge neutralization (f) consistent with $\hat{\nu}_b^2 > 0$ and $\hat{\nu}_e^2 > 0$, i.e., consistent with $(\hat{\omega}_{pb}^2/\omega_{\beta b}^{0^2})(1-\gamma_b^2 f) < 2\gamma_b^2$ and $0 \leqslant f < 1$. That is, Eq. (24) can be applied to the emittance-dominated, moderate-intensity ion beams $(\hat{\omega}_{pb}^2/\omega_{\beta b}^{0^2} \lesssim 0.2$, say) in the proton linacs and storage rings envisioned for the Spallation Neutron Source (SNS) and the Accelerator for Production of Tritium (APT). On the other hand, Eq. (24) can also be applied to the low-emittance, very high-intensity ion beams $(\hat{\omega}_{pb}^2/\omega_{\beta b}^{0^2}$ approaching $2\gamma_b^2$, for $f = 0)$ envisioned for heavy ion fusion [5].

A careful examination of Eq. (24) shows that the unstable, positive-frequency branch has frequency and wavenumber (ω, k_z) closely tuned to the values (ω_0, k_{z0}) defined by $\omega_0 = +\omega_e$ and $\omega_0 - k_{z0}V_b = -\omega_b$. In this regime, expressing $\omega = \omega_0 + \delta\omega$ and $k_z = k_{z0} + \delta k_z$, and assuming $|\delta\omega| \ll 2\omega_e$, the dispersion relation (24) is given to good approximation by

$$\delta\omega(\delta\omega - \delta k_z V_b)[1 - (\delta\omega - \delta k_z V_b)/2\omega_b] = -\Gamma_0^2 \equiv -\frac{\omega_f^4}{4\omega_e\omega_b}. \quad (26)$$

At moderate beam intensities with $\Gamma_0^2 \ll 1$, the unstable solution to Eq. (26) satisfies $|\delta\omega - \delta k_z V_b| \ll 2\omega_b$. In this regime, Eq. (26) can be approximated by the quadratic form $\delta\omega(\delta\omega - \delta k_z V_b) = -\Gamma_0^2 \equiv -\omega_f^4/4\omega_e\omega_b$. This quadratic dispersion relation supports an unstable solution with growth rate $\mathrm{Im}\,\delta\omega = \Gamma_0[1 - (\delta k_z V_b/2\Gamma_0)^2]^{1/2}$ for δk_z in the (symmetric) interval, $-2\Gamma_0 < \delta k_z V_b < 2\Gamma_0$. The maximum growth rate is $(\mathrm{Im}\,\delta\omega)_{\max} = \Gamma_0 \equiv \omega_f^2/2(\omega_e\omega_b)^{1/2}$, which occurs for $\delta k_z = 0$. The (stabilizing) influence of the conducting wall is minimized when $r_w^2/r_b^2 \to \infty$, in which case $(\mathrm{Im}\,\delta\omega)_{\max} = \Gamma_0$ reduces to

$$\frac{(\mathrm{Im}\,\delta\omega)_{\max}}{\omega_{\beta b}^0} = \frac{1}{2^{7/4}}\,\frac{f^{1/2}(\gamma_b m_b/Z_b m_e)^{1/4}(\hat{\omega}_{pb}^2/\omega_{\beta b}^{0^2})^{3/4}}{[1 + (f/2)\hat{\omega}_{pb}^2/\omega_{\beta b}^{0^2}]^{1/4}}. \quad (27)$$

For example, for a proton beam ($Z_b = 1$, $m_b/m_e = 1836$) with relativistic mass factor $\gamma_b = 1.85$, a moderate value of normalized beam intensity $\hat{\omega}_{pb}^2/\omega_{\beta b}^{0^2} = 0.1$, and fractional charge neutralization $f = 0.1$, Eq. (27) gives $(\mathrm{Im}\,\delta\omega)_{\max} = 0.127\omega_{\beta b}^0$, corresponding to a particularly virulent growth rate for the electron–proton (e-p) instability. For this choice of system parameters, the central oscillation frequency and wavenumber are $\omega_0 = 13.03\omega_{\beta b}^0$ and $k_{z0}V_b = 14.03\omega_{\beta b}^0$.

At the very high beam intensities of interest for heavy ion fusion, the transverse beam emittance

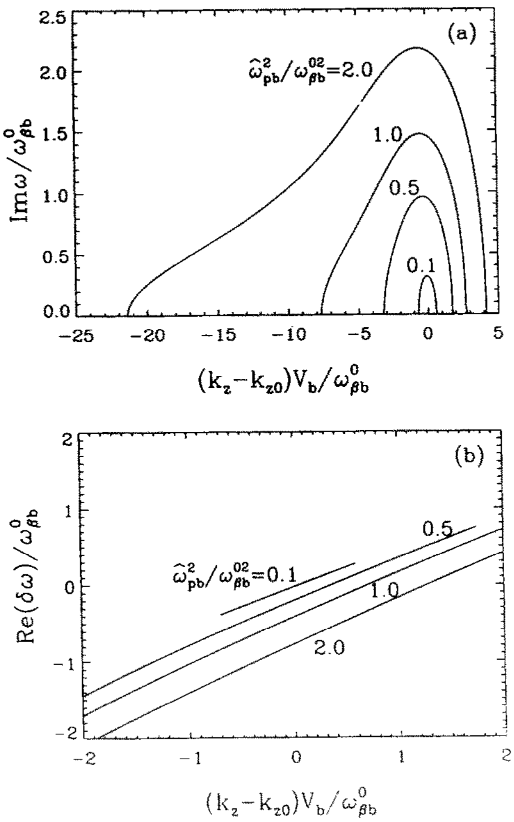

Fig. 1. Plots of (a) normalized growth rate $\mathrm{Im}\,\delta\omega/\omega^0_{\beta b}$, and (b) normalized real frequency $\mathrm{Re}\,\delta\omega/\omega^0_{\beta b}$ versus shifted axial wavenumber $(k_z - k_{z0})V_b/\omega^0_{\beta b}$ obtained from the dispersion relation (26) for the unstable branch with positive real frequency. System parameters correspond to $Z_b = 1$, $A = 200$ (cesium ions), $(\gamma_b - 1)m_b c^2 = 2.5$ GeV, $r_b/r_w = 0.5$, and $f = 0.1$. Curves are shown for several values of normalized beam intensity $\hat{\omega}^2_{pb}/\omega^{0^2}_{\beta b}$ ranging from 0.1 to 2.0.

(which is proportional to $\hat{T}_{\perp b}$) is very low, and the normalized beam intensity $\hat{\omega}^2_{pb}/\omega^{0^2}_{\beta b}$ can approach $2\gamma_b^2$ in the absence of background electrons ($f = 0$). This follows from the inequality $\hat{\nu}_b^2/\omega^{0^2}_{\beta b} = 2\hat{T}_{\perp b}/\gamma_b m_b \omega^{0^2}_{\beta b} r_b^2 \ll 1$ and the definition of $\hat{\nu}_b^2$ in Eq. (10). At such high beam intensities, it is necessary to solve the cubic dispersion relation (26) or the full quartic dispersion relation (24) for the complex oscillation frequency ω. Typical results obtained from Eq. (26) are illustrated in Fig. 1. Here, $(\mathrm{Im}\,\omega)/\omega^0_{\beta b}$ is plotted versus $(k_z - k_{z0})V_b/\omega^0_{\beta b}$ for several values of $\hat{\omega}^2_{pb}/\omega^{0^2}_{\beta b}$ ranging from 0.1 to 2.0. Other system parameters in Fig. 1 correspond to $Z_b = 1$, $A = 200$ (cesium ions), $(\gamma_b - 1)m_b c^2 = 2.5$ GeV, $r_b/r_w = 0.5$, and $f = 0.1$. For sufficiently small values of $\hat{\omega}^2_{pb}/\omega^{0^2}_{\beta b}$, the results obtained in Fig. 1 from the cubic dispersion relation (26) are in excellent agreement with the approximate quadratic dispersion relation. On the other hand, at very high beam intensity with $\hat{\omega}^2_{pb}/\omega^{0^2}_{\beta b} = 2$, say, it is evident from Fig. 1 that the growth rate $\mathrm{Im}\,\omega/\omega^0_{\beta b}$ has very large bandwidth, and becomes significantly skewed about $k_z = k_{z0}$. It is also striking from Fig. 1, that the instability growth rate can be very large for the very high beam intensities of interest for heavy ion fusion, e.g., $(\mathrm{Im}\,\omega)_{\max} = 2.17\omega^0_{\beta b}$, for $\hat{\omega}^2_{pb}/\omega^{0^2}_{\beta b} = 2$.

As a final point, it should be emphasized that the general kinetic eigenvalue equations (11)-(14) can be applied to electrostatic perturbations about a wide range of non-monoenergetic equilibrium distribution functions, $F_b^0(H_{\perp b})$ and $F_e^0(H_{\perp e})$, and corresponding self-consistent equilibrium density profiles, $n_b^0(r)$ and $n_e^0(r)$, that vary continuously with radial coordinate r. A detailed, self-consistent stability analysis based on Eqs. (11)-(14) for continuously varying equilibrium profiles is beyond the scope of the present article and will be the subject of a future investigation. For present purposes, it is sufficient to note that the spread in (depressed) betatron frequencies [11] associated with continuously varying equilibrium profiles is expected to lead to a *threshold* in beam intensity and/or fractional charge neutralization for the onset of the two-stream instability. By contrast, for the step-function density profiles considered here, the ion and electron betatron frequencies, $\hat{\nu}_b$ and $\hat{\nu}_e$, are *constant*, leading to sharply-defined particle resonances over the beam cross section, and a (correspondingly) strong version of the electron-ion two-stream instability.

This research was supported by the US Department of Energy and the APT Project and LANSCE Division of Los Alamos National Laboratory.

References

[1] R.C. Davidson, Physics of Nonneutral Plasmas (Addison-Wesley, Reading, MA, 1990), and references therein.

[2] T.P. Wangler, Principles of RF Linear Accelerators (John Wiley & Sons, New York, 1998).

[3] M. Reiser, Theory and Design of Charged Particle Beams (John Wiley & Sons, New York, 1994).

[4] R.A. Jameson, in: Advanced Accelerator Concepts, ed. J.S. Wurtele, Amer. Inst. of Phys. Conf. Proc. 279 (Amer. Inst. Phys., New York, 1993) p. 969.
[5] See, for example, Proc. 1995 Int. Symp. on Heavy Ion Inertial Fusion, eds. J.J. Barnard, T.J. Fessenden, E.P. Lee, J. Fusion Engineering and Design 32 (1996) 1–620, and references therein.
[6] T.-S. Wang, L. Smith, Part. Accel. 12 (1982) 247.
[7] J. Struckmeier, I. Hofmann, Part. Accel. 39 (1992) 219.
[8] R.C. Davidson, Physics of Plasmas 5 (1998) 3459, and references therein.
[9] R.C. Davidson, Phys. Rev. Lett. 81 (1998) 991.
[10] R.C. Davidson, C. Chen, Part. Accel. 59 (1998) 175.
[11] D.G. Koshkarev, P.R. Zenkevich, Part. Accel. 3 (1972) 1.
[12] E. Keil, B. Zotter, CERN Report CERN-ISR-TH/71-58 (1971).
[13] L.J. Laslett, A.M. Sessler, D. Möhl, Nucl. Instrum. Meth. 121 (1974) 517.
[14] R.C. Davidson, H.S. Uhm, Phys. Fluids 21 (1978) 60.
[15] D. Neuffer, E. Colton, D. Fitzgerald, T. Hardek, R. Hutson, R. Macek, M. Plum, H. Thiessen, T.-S. Wang, Nucl. Instrum. Meth. in Phys. Res. A 321 (1992) 1.
[16] D. Neuffer, C. Ohmori, Nucl. Instrum. Meth. in Phys. Res. A 343 (1994) 390.
[17] M.A. Plum, D.H. Fitzgerald, D. Johnson, J. Langenbrunner, R.J. Macek, F. Merrill, P. Morton, B. Prichard, O. Sander, M. Shulze, H.A. Thiessen, T.-S. Wang, C.A. Wilkinson, Proc. of the 1997 Particle Accelerator Conf. (1997) 1611.
[18] D. Sagan, A. Temnykh, Nucl. Instrum. Meth. in Phys. Res. A 344 (1994) 459.
[19] M. Izawa, Y. Sato, T. Toyomasu, Phys. Rev. Lett. 74 (1995) 5044.
[20] J. Byrd, A. Chao, S. Heifets, M. Minty, T.O. Roubenheimer, J. Seeman, G. Stupakov, J. Thomson, F. Zimmerman, Phys. Rev. Lett. 79 (1997) 79.
[21] K. Ohmi, Phys. Rev. E 55 (1997) 7550.
[22] See, for example, R.C. Davidson, Physics of Nonneutral Plasmas (Addison-Wesley, Reading, MA, 1990) pp. 240–271, and references therein.
[23] N.A. Krall, A.W. Trivelpiece, Principles of Plasma Physics (San Francisco Press, San Francisco, CA, 1986).
[24] See, for example, R.C. Davidson, Physics of Nonneutral Plasmas (Addison-Wesley, Reading, MA, 1990) Ch. 2, 4 and 10.
[25] R.C. Davidson, P.H. Stoltz, T.-S. Wang, Kinetic description of electron-proton instability in high-intensity proton linacs and storage rings based on the Vlasov-Maxwell equations, to be published.
[26] I. Kapchinskij, V. Vladimirskij, in: Proc. of the Int. Conf. on High Energy Accelerators and Instrumentation (CERN Scientific Information Service, Geneva, 1959) p. 274.